

# Ionization Process of Atoms by Intense Femtosecond Chirped Laser Pulses

Stéphane Laulan<sup>\*</sup>, Jérémie Haché, Harouna S. Ba, Samira Barmaki

Laboratoire de Physique Computationnelle et Photonique, Université de Moncton Campus de Shippagan, Shippagan, Canada  
Email: <sup>\*</sup>stephane.laulan@umoncton.ca

Received July 25, 2013; revised August 27, 2013; accepted September 26, 2013

Copyright © 2013 Stéphane Laulan *et al.* This is an open access article distributed under the Creative Commons Attribution License, which permits unrestricted use, distribution, and reproduction in any medium, provided the original work is properly cited.

## ABSTRACT

We numerically investigate the ionization mechanism in a real hydrogen atom under intense fem to second chirped laser pulses. The central carrier frequency of the pulses is chosen to be 6.2 eV ( $\lambda = 200$  nm), which corresponds to the fourth-harmonic of the Ti:Sapphire laser. Our simulation of the laser-atom interaction consists on numerically solving the three-dimensional time-dependent Schrödinger equation with a spectral method. The unperturbed wave functions and electronic energies of the atomic system were found by using an  $L^2$  discretization technique based on the expansion of the wave functions on B-spline functions. The presented results of kinetic energy spectra of the emitted electrons show the sensitivity of the ionization process to the chirp parameter. Particular attention is paid to the important role of the excited bound states involved in the ionization paths.

**Keywords:** Hydrogen Atom; Chirped Laser; Multiphoton Ionization; Population Transfer; Nonperturbative Approach

## 1. Introduction

The continuous progress in intense and short laser pulses generation techniques has led to extensive experimental and theoretical investigations on how to use these pulses as tools to control the ultra fast electron dynamic in atomic and molecular systems [1-3]. Recently, physicists took an interest in using chirped laser pulses to investigate laser-matter interactions. These pulses are efficient to control the ionization and excitation mechanisms when compared with unchirped laser pulses, *i.e.* transform-limited laser pulses [4-9]. The ability to control population transfer from an initial state to a desired final state is of crucial importance as it will open the way to the control of the product yields in chemical reactions.

The most known nonlinear processes that arise in ultra fast laser-matter interactions will change when intense and short chirped laser pulses are used instead of the transform-limited laser pulses [10-14]. The above-threshold ionization (ATI) process is the most important and well-understood nonlinear process by physicists. It is the signature that atoms or molecules can absorb more photons than is strictly necessary for the ionization to occur. The shape of the ATI spectrum, *i.e.*, the kinetic energy spectrum of the emitted electrons, exhibits a series of

peaks equally separated by the absorbed incident photon frequency [15-18].

In this paper, we point out the effect of the laser chirp parameter on the kinetic energy spectra of the emitted electrons from the hydrogen atom. We used intense femtosecond chirped laser pulses of central carrier frequency  $\omega_0 = 6.2$  eV, which corresponded to the fourth-harmonic of the Ti:Sapphire laser. A chirped laser pulse is experimentally produced by chirp filtering of a transform-limited laser pulse. We consider, in this paper, a realistic experimental representation of a linearly polarized chirped laser pulse, in which the chirp parameter increases the time duration of the original transform-limited laser pulse and decreases its intensity. The frequency bandwidth of the resulting chirped pulse remains the same as that of the corresponding transform-limited laser pulse. The theoretical approach we used to calculate the unperturbed energetic structure of the hydrogen atom is based on an  $L^2$  discretization technique using B-spline functions [19,20]. The kinetic energy spectra of the emitted electrons were generated by numerically solving the three-dimensional time-dependent Schrödinger equation using a spectral method [21-23]. We follow in time the transfer of the population to the intermediate bound states involved in the ionization paths. We examine then the sensitivity of the excitation mechanism to the sign of the chirp pa-

<sup>\*</sup>Corresponding author.

parameter and how that affects the kinetic energy spectra of the emitted electrons.

Atomic units (a.u.) are used throughout the paper unless otherwise mentioned.

## 2. Theoretical Approach

### 2.1. Atomic Structure Calculations

The time-independent Schrödinger equation (TISE) describing the electron motion around the atomic nucleus is given by:

$$(H_0 - E_{nlm})\phi_{nlm}(r) = 0. \quad (1)$$

$H_0$  is the nonrelativistic field-free Hamiltonian in spherical coordinates, which reads

$$H_0 = -\frac{1}{2}\nabla^2 + \frac{1}{r} = -\frac{1}{2}\left[\frac{1}{r^2}\frac{\partial}{\partial r}\left(r^2\frac{\partial}{\partial r} - \frac{l(l+1)}{2r^2}\right)\right] + \frac{1}{r}. \quad (2)$$

For a given electron angular momentum  $l$  and projection  $m$ , the solution of Equation (1) can be written as follows:

$$\phi_{nlm}(r) = \sum_{i=1}^{N_b} C_i^{nlm} \frac{B_i^k(r)}{r} Y_l^m(\theta, \phi). \quad (3)$$

$Y_l^m(\theta, \phi)$  is the spherical harmonic functions depending on angular coordinates. The B-spline function of order  $k$  denoted by  $B_i^k(r)$  is a piecewise polynomial of degree  $k-1$  [20]. We use  $N_b$  B-spline functions, that are distributed along the radial axis, in a radial box defined from  $r=0$  to  $R_{\max}$ . A direct diagonalization of Equation (1) gives the unperturbed eigenenergies  $E_{nlm}$  and eigenfunctions of all bound and continuum discretized states. We have proven the efficiency of our discretization technique in previous works on two-active electron systems [21-23].

### 2.2. Time-Dependent Calculations

Within the electric dipole approximation, the time-dependent Schrödinger equation (TDSE) describing the electron motion in the presence of the laser field is given by:

$$i\frac{\partial}{\partial t}\Psi(\mathbf{r}, t) = [H_0(\mathbf{r}) + H_{\text{int}}(\mathbf{r}, t)]\Psi(\mathbf{r}, t). \quad (4)$$

$H_{\text{int}}(\mathbf{r}, t)$  describes the interaction of the electron with the laser field. It could be expressed in different gauges as for example the length or velocity gauges. As we adopt here the velocity gauge,  $H_{\text{int}}(\mathbf{r}, t)$  is written as the scalar product of the potential vector and the electron momentum:

$$H_{\text{int}}(\mathbf{r}, t) = -i\mathbf{A}(t, \xi) \cdot \nabla, \quad (5)$$

where  $\mathbf{A}(t, \xi)$  is the vector potential of the chirped laser pulse linearly polarized along the  $z$  axis.

The time-dependent total wave function  $\Psi(\mathbf{r}, t)$  in Equation (4) is expanded on the basis of the field-free atomic eigenstates, normalized to unity,

$$\Psi(\mathbf{r}, t) = \sum_{nlm} f^{nlm}(t) \exp(-iE_{nlm}t) \phi_{nlm}(\mathbf{r}). \quad (6)$$

By substituting Equation (6) into Equation (4), we obtain a set of coupled integro-differential equations, which we solved using an explicit fifth-order Runge-Kutta numerical method [21].

The vector potential of the chirped laser pulse considered here is given by:

$$\mathbf{A}(t, \xi) = A(\xi)F(t, \xi)\sin(\omega(t, \xi)t + \varphi)\mathbf{e}_z, \quad (7)$$

With  $\xi$  is the chirp parameter,  $\varphi$  the pulse carrier-envelope phase (CEP),  $A(\xi)$  the peak amplitude,  $\omega(t, \xi)$  the instantaneous frequency and  $F(t, \xi)$  the Gaussian time envelope. We note that, in experiment, chirp filters are implemented by use of dispersive optical systems. Upon transmission through a filter characterized by a  $b$  chirp coefficient, an initially transform-limited pulse ( $\xi=0$ ) becomes chirped, *i.e.*, with frequency  $\omega(t, \xi)$  that varies in time and depends on the chirp parameter  $\xi = b/\tau_0^2$  (for the experimental details see [24]).  $\tau_0$  is the full width at half maximum (FWHM) duration of the transform-limited pulse. The filtered pulse will be up-chirped if  $\xi$  is positive and will be down-chirped if  $\xi$  is negative.

The expression of  $A(\xi)$  is given by :

$$A(\xi) = \frac{E(\xi)}{\omega_0}, \quad (8)$$

where  $E(\xi) = \sqrt{I(\xi)/I_{\text{au}}}$  is the electric field amplitude of the chirped pulse, with  $I_{\text{au}} = 3.51 \times 10^{16}$  W·cm<sup>-2</sup> the atomic unit of intensity and  $\omega_0$  the central carrier frequency. The intensity of the chirped pulse  $I(\xi)$  is related to the intensity  $I_0$  of the transform-limited pulse ( $\xi=0$ ) by:

$$I(\xi) = \frac{I_0}{\sqrt{1+\xi^2}}. \quad (9)$$

The instantaneous frequency  $\omega(t, \xi)$  and the Gaussian time envelope  $F(t, \xi)$  are given, respectively, by :

$$\omega(t, \xi) = \omega_0 + 4 \ln 2 \frac{\xi t}{(1+\xi^2)\tau_0^2} \quad (10)$$

and

$$F(t, \xi) = \exp\left[-4 \ln 2 \frac{t^2}{(1+\xi^2)\tau_0^2}\right], \quad (11)$$

The FWHM duration of the chirped pulse is given by:

$$\tau(\xi) = \tau_0 \sqrt{1 + \xi^2}. \quad (12)$$

At the switch-off of the laser pulse ( $t = t_{final}$ ), the probability of finding the system in the  $\phi_{nlm}(r)$  electronic eigenstate is given by:

$$P_{nlm} = \left| \left\langle \phi_{nlm}(r) \left| \Psi(r, t_{final}) \right. \right\rangle \right|^2. \quad (13)$$

The kinetic energy spectrum of the emitted electrons is calculated as follows:

$$\frac{dP}{dE} = \rho(E) \sum_{nlm, E > 0} \left| \left\langle \phi_{nlm}(r) \left| \Psi(r, t_{final}) \right. \right\rangle \right|^2, \quad (14)$$

with  $\rho(E)$  the density of continuum states [20].

### 3. Results and Discussions

For the numerical calculations, we have considered a set of  $N_b = 1200$  B-splines of order  $k = 7$  defined on the radial box of maximum length  $R_{max} = 1000$  a.u.. We have fixed the maximum electron angular momentum to  $l = 12$ . As we choose the laser pulse to be polarized linearly along the  $z$  axis, only electronic transitions between states of  $m = 0$  magnetic quantum number are permitted. We kept in all our calculations the CEP constant and set to  $\varphi = 0$ . The convergence of our numerical results has been checked by increasing the number of B-spline functions, the radial box size and the number of angular momentum  $l$ . We have also checked that the results are gauge independent.

We consider in this paper a transform-limited pulse ( $\xi = 0$ ) of central carrier frequency  $\omega_0 = 0.228$  a.u. (6.2 eV), which corresponds to the fourth-harmonic of Ti:Sa laser ( $\lambda = 200$  nm). The pulse has an intensity  $I_0 = 10^{14}$  W·cm<sup>-2</sup> and a FWHM duration  $\tau_0 = 137.79$  a.u. = 3.33 fs.

We plot in **Figure 1** the transform-limited pulse vector potential  $A(t, \xi = 0)$  variation with time. We compare in the same figure  $A(t, \xi = 0)$  with the vector potentials of a simulated filtered up-chirped pulse of  $\xi = +1$  and a down-chirped pulse of  $\xi = -1$ . Both chirped pulses, according to Equations (9) and (12), have an intensity of  $I(\xi = \pm 1) = 7.08 \times 10^{13}$  W·cm<sup>-2</sup> and a FWHM duration  $\tau(\xi = \pm 1) = 194.8$  a.u. = 4.7 fs. The form of the vector potential used in this paper (see Equation (7)) simulates a realistic experimental case in which the chirp filtering decreases the intensity of the transform-limited pulse and increases its total duration. We also present in **Figure 1** the spectral profile of the three pulses and the variation of their instantaneous frequency  $\omega(t, \xi)$  with time. Specifically, an up-chirped pulse (down-chirped) with a positive (negative) value of  $\xi$  means that the instantaneous laser frequency increases (decreases) with time. Nevertheless, the frequency bandwidth of the up- and down-chirped pulses remains the same as that of the transform-limited pulse.

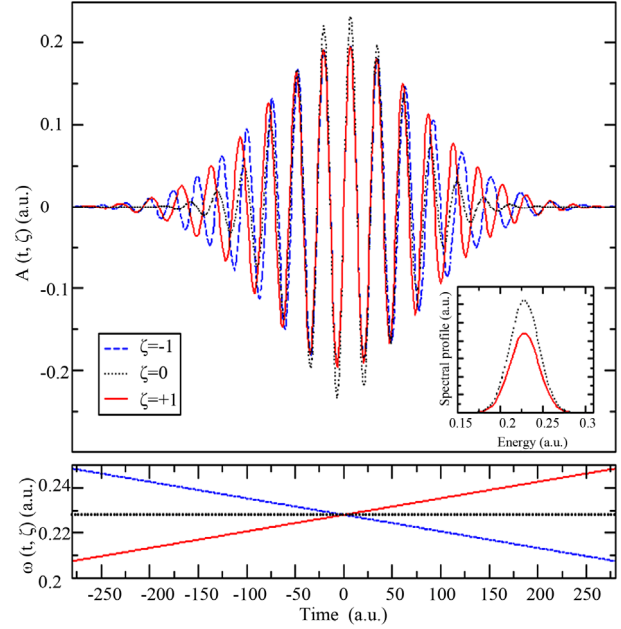


**Figure 1.** Dependence of laser pulse vector potential  $A(t, \xi)$ , spectral profile and instantaneous frequency  $\omega(t, \xi)$  on the chirp parameter  $\xi = -1, 0, +1$ . The chirped pulses ( $\xi = \pm 1$ ) have a central carrier frequency  $\omega_0 = 0.228$  a.u. (6.2 eV), CEP  $\varphi = 0$ , intensity  $I(\xi) = I_0 / \sqrt{1 + \xi^2}$  and FWHM duration  $\tau(\xi) = \tau_0 \sqrt{1 + \xi^2}$ , where  $I_0 = 10^{14}$  W·cm<sup>-2</sup> and  $\tau_0$  are respectively the intensity and the FWHM duration of the transform-limited pulse ( $\xi = 0$ ).

We submit the hydrogen atom to each of three pulses showed in **Figure 1**. In **Figure 2**, we compare in logarithmic scale the kinetic energy spectra of the emitted electrons we obtained at the end of each pulse interaction with the atom. The spectra exhibit a number of peaks that are the signature of the ATI nonlinear process by which the atom, under these intense laser pulses, has absorbed  $S$  more photons than the minimum number of three photons necessary to reach the ionization limit ( $I_p = 0.5$  a.u. = 13.6 eV). The many peaks observed in kinetic energy spectra of the emitted electrons have relatively narrow widths, and are centered on electronic energies  $E^S$  given by:

$$E^S = (3 + S)\hbar\omega - I_p + U_p, \quad (15)$$

where  $U_p = I/4\omega^2 I_{au}$  is the electron ponderomotive energy. The hydrogen atom under a strong pulse of intensity  $I$  and photon frequency  $\omega$  experiences an ionization potential increase of  $U_p$ .

We notice in **Figure 2** that a nonzero chirp value affects the height and position of the peaks. The down-chirped pulse (up-chirped pulse) moves slightly the ATI peaks to the left (right) when compared to the unchirped pulse. The modification in the ATI shape and properties is a result of

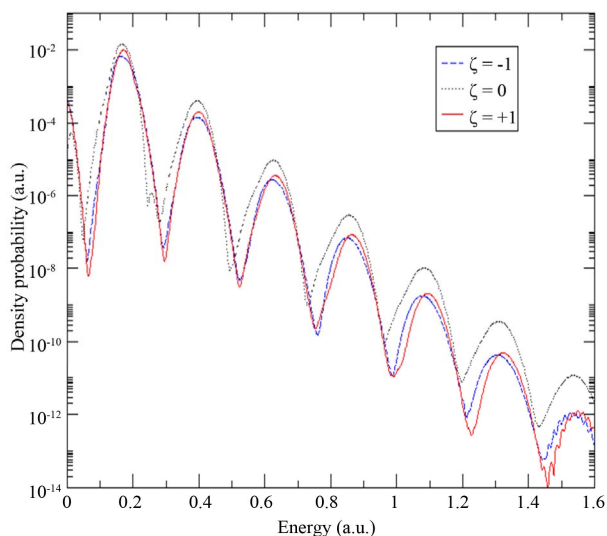


**Figure 2.** Kinetic energy spectra of the emitted electrons obtained at the end of chirped pulses with  $\xi = -1$  (dashed line),  $\xi = 0$  (dotted line) and  $\xi = +1$  (solid line) in logarithmic scale (1 a.u. of energy is equivalent to 27.2 eV).

how the sign of the chirp influences the time variation of the instantaneous frequency  $\omega(t, \xi)$ , which affects the energy shift of the excited states and then the energy of emitted electrons.

Let us now observe more precisely if the sensitivity of the ionization process will persist for other chirp parameter values. In **Figures 3(a)-(d)**, we present in nonlogarithmic scale the first peak  $S = 0$  of the emitted electron energy spectrum which is due to the ionization of the atom with three photons. The results were obtained at the end of the laser pulses with the following chirp parameters  $\xi = \pm 0.5, \pm 1, \pm 1.5, \pm 2$ . We compare in each case the chirped pulses ( $\pm \xi$ ) results with that obtained with the unchirped pulse  $\xi = 0$ . In the first case ( $\xi = \pm 0.5$ ), the intensity of the up- and down-chirped pulses is  $I(\xi = \pm 0.5) = 8.9 \times 10^{13} \text{ W}\cdot\text{cm}^{-2}$  and their FWHM duration is  $\tau(\xi = \pm 0.5) = 154 \text{ a.u.} = 3.7 \text{ fs}$ . In the second case ( $\xi = \pm 1$ ), the intensity and the FWHM duration of the chirped pulses are the same used previously. In the third case,  $I(\xi = \pm 1.5) = 5.5 \times 10^{13} \text{ W}\cdot\text{cm}^{-2}$  and  $\tau(\xi = \pm 1.5) = 248 \text{ a.u.} = 6 \text{ fs}$ . Finally, in the fourth case,

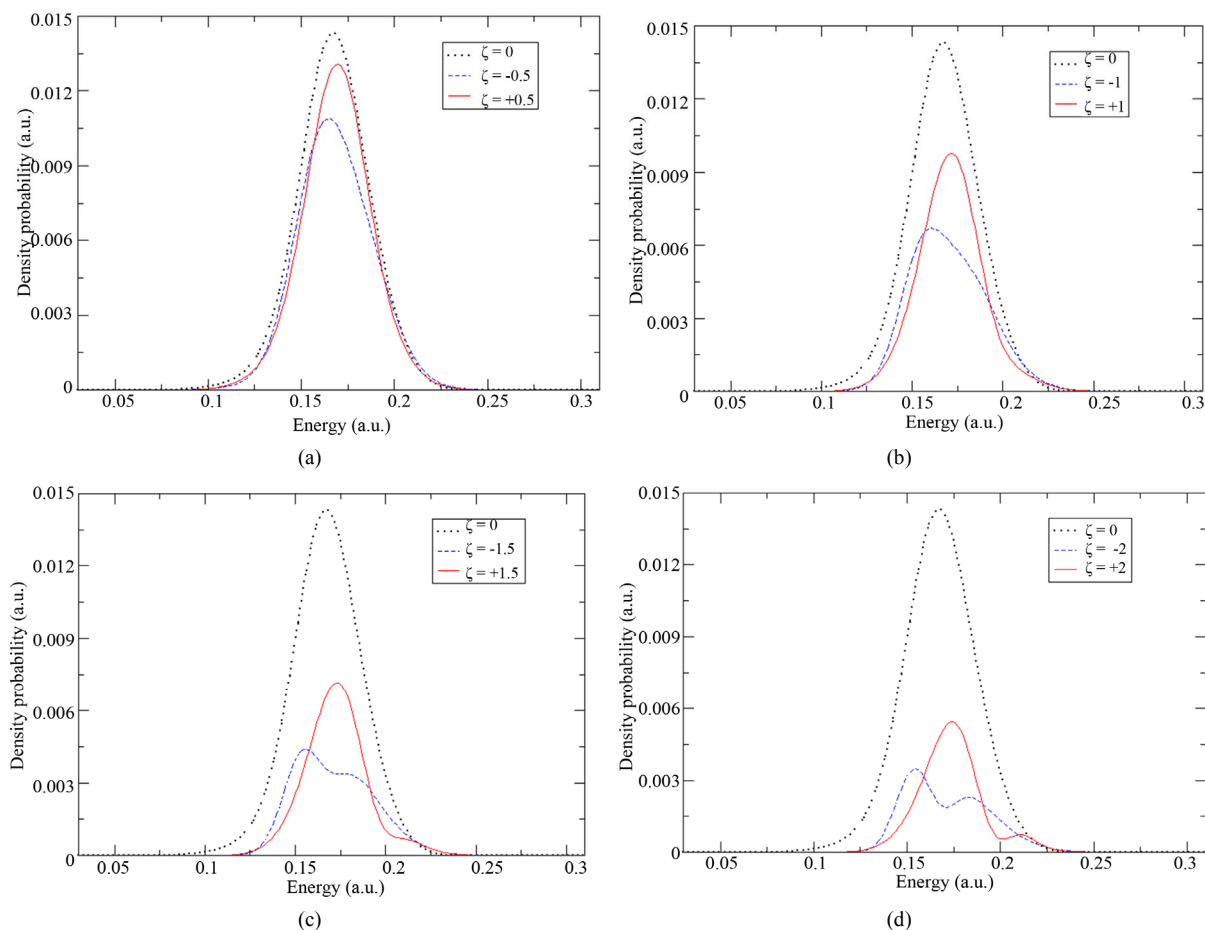


**Figure 3.** Peaks  $S = 0$  of the emitted electron energy spectrum obtained at the end of laser pulses with (a)  $\xi = 0, \pm 0.5$ ; (b)  $\xi = 0, \pm 1$ ; (c)  $\xi = 0, \pm 1.5$  and (d)  $\xi = 0, \pm 2$  in nonlogarithmic scale. Solid line (dashed line) corresponds to the results obtained with a positive (negative) chirp parameter, and dotted line with  $\xi = 0$ .

the intensity decreases to

$I(\xi = \pm 2) = 4.5 \times 10^{13} \text{ W}\cdot\text{cm}^{-2}$  and the duration increases to  $\tau(\xi = \pm 2) = 308 \text{ a.u.} = 7.45 \text{ fs}$ .

When we compare between the results presented in **Figure 3**, we first notice that in each of the four cases, the emitted electron energy spectrum obtained with the unchirped pulse has higher magnitude than those obtained with the chirped laser pulses, which is expected as the intensity of unchirped pulse is higher than that of chirped pulses. Secondly, the increasing of  $|\xi|$  seems to produce only a slight Stark shift of the emitted electron spectrum towards higher electronic energies when the atom is under the up-chirped pulse. In contrast, when the atom is submitted to the down-chirped pulse, we observe a slight energy shift towards lower electronic energies with, however, a visible break-up of the ionization peak into two narrow peaks.

The significant change in the shape of the emitted electron energy spectra, particularly with a down-chirped laser pulse, results from the sensitivity of the excitation process to the sign of the chirp parameter. The latter affects the average of the population transferred to the intermediate bound states involved in the ionization paths. To prove the role of the excited bound states in this study, we removed them all from the atomic basis set and then we solved the TDSE. We have found that the chirp influence on ATI spectra has totally disappeared.

**Figure 4** indicates the excitation scheme induced by the laser frequency  $\omega_0 = 0.228 \text{ a.u.}$ . To understand the influence of the chirp parameter on the excitation mechanism, we have examined how the population of the excited states by the up-chirped laser pulse takes place compared to the down-chirped pulses. We followed in time the population of the  $2s$ ,  $2p$ ,  $3s$ ,  $4s$ ,  $3d$  and  $4d$  bound states in the presence of the chirped pulses of

$\xi = \pm 0.5, \pm 1, \pm 1.5, \pm 2$  used previously. We found that the  $2s$  and  $2p$  bound electronic states, off-resonance, are not affected by the chirp in contrast with the  $3s$ ,  $4s$ ,  $3d$  and  $4d$  states that are close to resonance by two-photon transition from the  $1s$ . We also found that the  $3d$  and  $4d$  excited states are much more populated than the  $3s$  and  $4s$  states. The ionization occurs mostly by electrons transition from the  $3d/4d$  ( $l=2$ ) states to the  $nf$  ( $l=3$ ) continuum channel and feebly from the  $3s/4s$  ( $l=0$ ) states to the  $np$  ( $l=1$ ) continuum channel.

So, we only report in **Figure 5** the time evolution of the  $3d$  and  $4d$  bound states population. We notice that the population of the  $3d$  state decreases when we increase the chirp parameter and also that the down-chirp pulse populates the  $4d$  state more than an up-chirped pulse does. During its time duration, an up-chirped pulse induces a two-photon resonant transition from the fundamental state  $1s$  to the  $3d$  first and from  $1s$  to the  $4d$  later in time. In contrast, a down-chirped pulse induces a two-photon

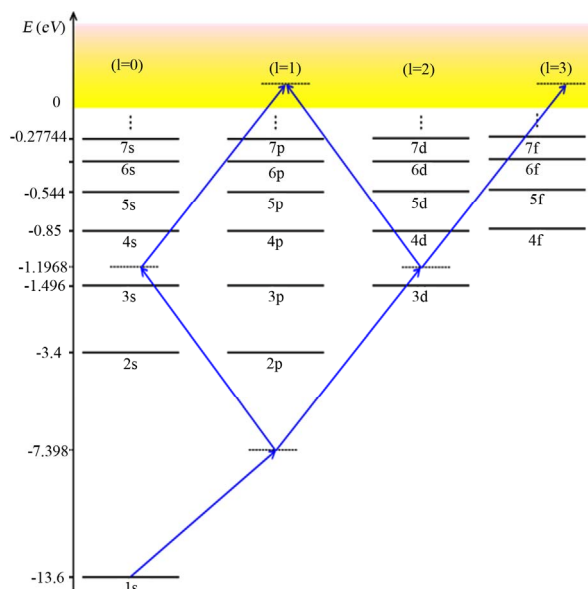


**Figure 4. Schematic hydrogen atom energy level diagram showing the ionization paths with a laser pulse of central carrier frequency  $\omega_0 = 0.228 \text{ a.u.}$ .**

resonant transition from the  $1s$  to the  $4d$  first and from  $1s$  to the  $3d$  later in time. That explains why in **Figure 5** the  $4d$  state is more(less) populated when the atom is under down-chirped (up-chirped) pulse.

The double peaks structure observed in **Figures 3(c)** and **(d)**, when we fix the value of the chirp parameter to  $\xi = -1.5$  and  $-2$ , is essentially due to two factors. The first is by increasing  $|\xi|$ , we decrease the laser intensity, so the population of the  $3d$  state decreases as it becomes then less coupled to  $1s$  by resonant two-photon transition. The second is a chirped pulse with a negative  $\xi$  increases the population of the  $4d$  state. Ionization, in this case, occurs by the transfer of the population from both the  $3d$  and  $4d$  states to the  $nf$  ( $l=3$ ) continuum channel causing the appearance of the two narrow peaks observed in the emitted electron energy spectra. In contrast with the case when we decrease (increase) the chirp parameter (laser intensity), see **Figures 3(a)** and **(b)**, here the transfer of the population occurs predominantly from the most populated  $3d$  state to the continuum. Here, no double narrow peaks structure is observed.

The excitation mechanism could be controlled by chirped laser pulses. By varying the sign of the chirp parameter, the instantaneous frequency changes in time differently, which induces different excitation scenarios. With chirped laser pulses, we could determine which level will have a bigger average population during the laser-atom interaction and thus control the ionization yield. We have investigated the sensitivity of the ionization process to the chirp parameter for various other harmonic frequencies of Ti:Sa laser. We have observed that the sensitivity is generally more accentuated when the chirp

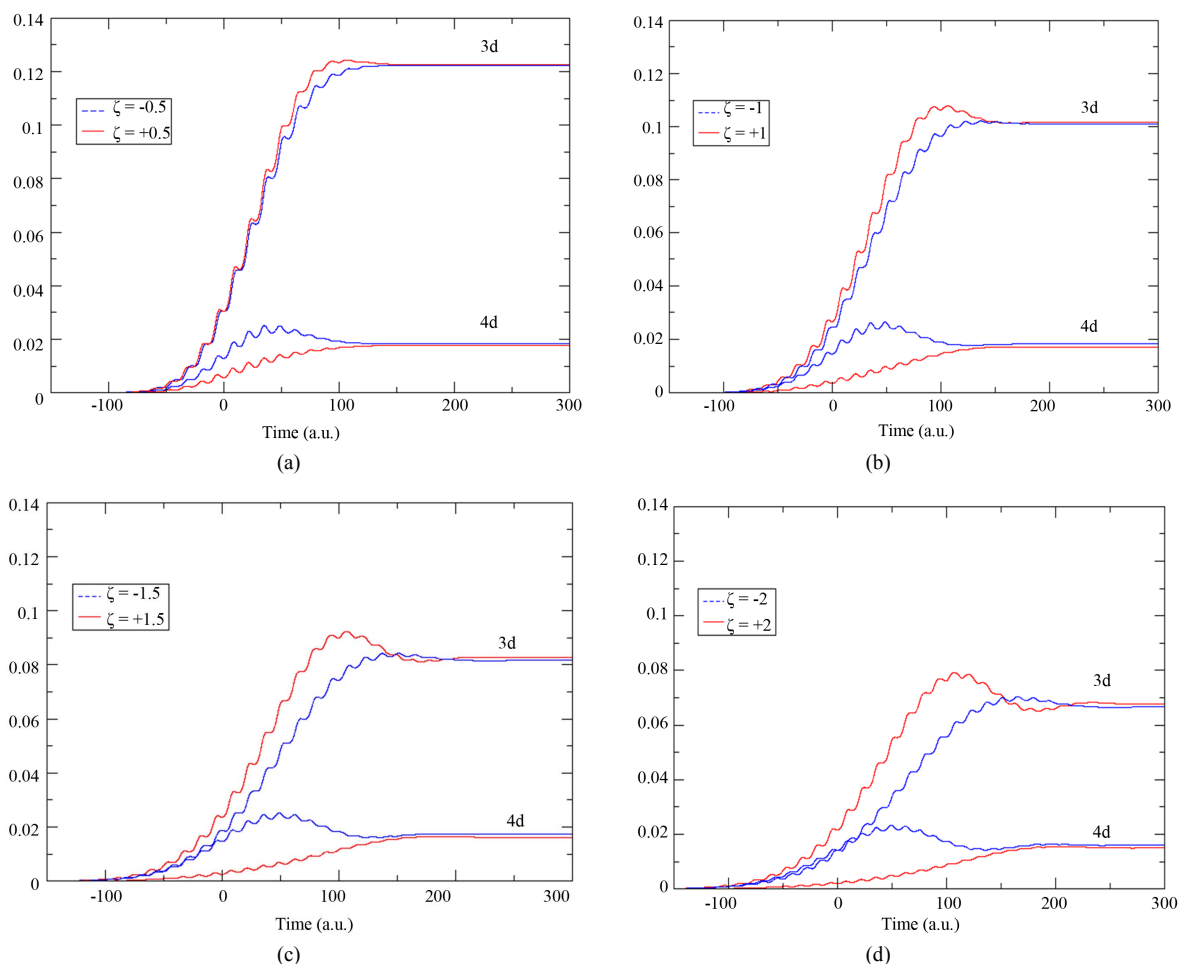


**Figure 5.** Population of the  $3d$  and  $4d$  bound states in the presence of up-chirped (solid line) and down-chirped (dashed line) laser pulses of (a)  $\zeta = \pm 0.5$ ; (b)  $\zeta = \pm 1$ ; (c)  $\zeta = \pm 1.5$  and (d)  $\zeta = \pm 2$ .

induces resonant transitions in the excitation mechanism.

#### 4. Conclusion

We have presented in this paper the results of numerical calculations of the emitted electron energy spectra in the hydrogen atom under intense fem to second chirped laser pulses. We have observed that the ionization and excitation dynamics are very sensitive to the chirp parameter. Intense ultra short chirped laser pulses could be an important tool to study image and control the electron dynamic in atoms and molecules. The study presented in this paper could be applicable to control the transfer or the inversion of the population in another atomic target. The chirp dependence of the emitted electron energy spectra observed here may prove useful for experimental characterization of chirped laser pulses.

#### 5. Acknowledgements

The present research was supported by the NSERC and by the New Brunswick Innovation Foundation (NBIF).

Allocation of CPU time and assistance with the computer facilities from the Atlantic Computational Excellence Network (ACE net, St-John's, NL, Canada) and from the "Réseau Québécois de Calcul de Haute Performance" are acknowledged.

#### REFERENCES

- [1] J. C. Diels and W. Rudolph, "Ultrashort Laser Pulse Phenomenon: Fundamentals, Techniques and Applications on Femtosecond Time Scale," Academic Press, New York, 1996.
- [2] P. Agostini and L. F. DiMauro, *Reports on Progress in Physics*, Vol. 67, 2004, pp. 813-855. <http://dx.doi.org/10.1088/0034-4885/67/6/R01>
- [3] K. Yamanouchi, S. L. Chin, P. Agostini and G. Ferrante, "Progress in Ultrafast Intense Laser Science III," Springer-Verlag, New York, 2007.
- [4] R. B. Vrijen, D. I. Duncan and L. D. Noordam, *Physical Review A*, Vol. 56, 1997, pp. 2205-2212. <http://dx.doi.org/10.1103/PhysRevA.56.2205>
- [5] K. J. Schafer and K. C. Kulander, *Laser Physics*, Vol. 7,

- 1997, pp. 740-750.
- [6] J. Cao, C. J. Barden and K. R. Wilson, *Journal of Chemical Physics*, Vol. 113, 2000, pp. 1898-1909. <http://dx.doi.org/10.1063/1.481993>
- [7] J. Lambert, M. W. Noel and T. F. Gallagher, *Physical Review A*, Vol. 66, 2002, Article ID: 053413. <http://dx.doi.org/10.1103/PhysRevA.66.053413>
- [8] C. W. S. Conover, M. C. Doogue and F. J. Struwe, *Physical Review A*, Vol. 65, 2002, Article ID: 033414. <http://dx.doi.org/10.1103/PhysRevA.65.033414>
- [9] V. Prasad, B. Dahija and K. Yamashita, *Physica Scripta*, Vol. 82, 2010, Article ID: 055302. <http://dx.doi.org/10.1088/0031-8949/82/05/055302>
- [10] Marani and E. J. Robinson, *Journal of Physics B*, Vol. 32, 1999, pp. 711-736. <http://dx.doi.org/10.1088/0953-4075/32/3/014>
- [11] J. Wu, G. T. Zhang, C. L. Xia and X. S. Liu, *Physical Review A*, Vol. 82, 2010, Article ID: 013411.
- [12] J. J. Carrera and S. I. Chu, *Physical Review A*, Vol. 75, 2007, Article ID: 033807. <http://dx.doi.org/10.1103/PhysRevA.75.033807>
- [13] T. Nakajima, *Physical Review A*, Vol. 75, 2007, Article ID: 053409. <http://dx.doi.org/10.1103/PhysRevA.75.053409>
- [14] Y. Xiang, Y. Niu and S. Gong, *Physical Review A*, Vol. 80, 2009, Article ID: 023423. <http://dx.doi.org/10.1103/PhysRevA.80.023423>
- [15] P. Agostini, F. Fabre, G. Mainfray, G. Petite and N. K. Rahman, *Physical Review Letters*, Vol. 42, 1979, pp. 1127-1130. <http://dx.doi.org/10.1103/PhysRevLett.42.1127>
- [16] J. Javanainen, J. H. Eberly and Q. Su, *Physical Review A*, Vol. 38, 1988, pp. 3430-3446. <http://dx.doi.org/10.1103/PhysRevA.38.3430>
- [17] W. Becker, F. Grasbon, R. Kopold, D. B. Milosevic, G. G. Paulus and H. Walther, *Advances in Atomic Molecular and Optical Physics*, Vol. 48, 2002, pp. 35-98. [http://dx.doi.org/10.1016/S1049-250X\(02\)80006-4](http://dx.doi.org/10.1016/S1049-250X(02)80006-4)
- [18] R. R. Freeman, P. H. Bucksbaum, H. Milchberg, S. Darack, D. Schumacher and M. E. Geusic, *Physical Review Letters*, Vol. 59, 1987, pp. 1092-1095. <http://dx.doi.org/10.1103/PhysRevLett.59.1092>
- [19] C. de Boor, "A Practical Guide to Splines," Springer-Verlag, New York, 1978. <http://dx.doi.org/10.1007/978-1-4612-6333-3>
- [20] H. Bachau, E. Cormier, P. Decleva, J. E. Hansen and F. Martin, *Reports on Progress in Physics*, Vol. 64, 2001, pp. 1815-1943. <http://dx.doi.org/10.1088/0034-4885/64/12/205>
- [21] S. Laulan and H. Bachau, *Physical Review A*, Vol. 68, 2003, Article ID: 013409. <http://dx.doi.org/10.1103/PhysRevA.68.013409>
- [22] S. Laulan and H. Bachau, *Physical Review A*, Vol. 69, 2004, Article ID: 033408. <http://dx.doi.org/10.1103/PhysRevA.69.033408>
- [23] E. Fomouo, S. Laulan, B. Piraux and H. Bachau, *Journal of Physics B*, Vol. 39, 2006, pp. S427-S435.
- [24] B. E. A. Saley and M. C. Teich, "Fundamentals of Photonics," John Wiley and Sons Inc., Hoboken, 2007.